J. Fluid Mech. (2011), *vol.* 687, *pp.* 529–539. © Cambridge University Press 2011
doi:10.1017/jfm.2011.388

Linear stability of double-diffusive two-fluid channel flow

Kirti Chandra Sahu[1]† **and Rama Govindarajan**[2]

[1] Department of Chemical Engineering, Indian Institute of Technology Hyderabad, Yeddumailaram 502 205, India

[2] Engineering Mechanics Unit, Jawaharlal Nehru Centre for Advanced Scientific Research, Jakkur, Bangalore 560 064, India

(Received 30 May 2011; revised 8 September 2011; accepted 9 September 2011; first published online 14 October 2011)

Double-diffusive density stratified systems are well studied and have been shown to display a rich variety of instability behaviour. However double-diffusive systems where the inhomogeneities in solute concentration are manifested in terms of stratified viscosity rather than density have been studied far less and, to the best of the authors' knowledge, not in high-Reynolds-number shear flows. In a simple geometry, namely the two-fluid channel flow of such a system, we find a new double-diffusive mode of instability. The instability becomes stronger as the ratio of diffusivities of the two scalars increases, even in a situation where the net Schmidt number decreases. The double-diffusive mode is destabilized when the layer of viscosity stratification overlaps with the critical layer of the perturbation.

Key words: double diffusive convection, multiphase flow, transition to turbulence

1. Introduction

The stability of miscible two-fluid flow has been extensively studied experimentally, theoretically and numerically, primarily due to its relevance in practical applications such as the transportation of crude oil in pipelines (Joseph *et al.* 1997). An understanding of the stability of two-layer or multilayer flows is essential in chemical industry, to determine, for example, the degree of mixing. In these flows, fluid properties vary with position and time due to concentration variations of the multiple species present. We are interested here in a system containing two diffusing species. When the two species have sharply different rates of diffusion, unexpected dynamics can be displayed. An extremely well-studied system of this type is that of a double-diffusive (DD) fluid where the viscosity is constant but density depends on the concentrations of both species (see, e.g., Turner 1974; Huppert 1971; May & Kelley 1997). Here one can have a rich array of instabilities when an equivalent single-component (SC) system would be stable. The fingering instability is a commonly quoted example of this type. This instability occurs when salt and temperature concentrations are stratified in water such that we have warm, salty water lying above cool, fresh water with density increasing in the direction of gravity, i.e. being nominally 'stably' stratified. In contrast the consequences of viscosity being stratified

† Email address for correspondence: ksahu@iith.ac.in

https://doi.org/10.1017/jfm.2011.388 Published online by Cambridge University Press

rather than density have only been very sparingly explored. To the best of the authors' knowledge, studies of this aspect are rather recent, and have focused on porous media (e.g. Pritchard 2004, 2009), and chemically driven systems (Nagatsu *et al.* 2007; Podgorski *et al.* 2007; Swernath & Pushpavanam 2007; Grosfils *et al.* 2009; Hejazi *et al.* 2010). In the former, by conducting numerical simulations, Mishra *et al.* (2010) found DD instability in a classically stable system of a more viscous fluid displacing a less viscous fluid.

To the best of the authors' knowledge, the stability of inertial flows of DD systems with varying viscosity has not been studied before. We therefore study here the linear stability of one of the simplest shear flows of a DD system, namely symmetric three-layer pressure-driven flow through a two-dimensional channel, and find a DD mode of instability. The layers close to the centreline and close to the wall contain different constant-property fluids, and there is a mixed layer between the two where the viscosity varies smoothly. The system may be taken to consist of a solvent with two solutes dissolved in it, with one of them diffusing faster than the other. Pure solvent would occupy the core region, for example, and a solution of known concentrations of the two solutes would occupy the neighbourhood of the wall.

The equivalent SC system has been studied by several authors, e.g. Ranganathan & Govindarajan (2001), Ern, Charru & Luchini (2003) and Malik & Hooper (2005). Some salient earlier studies of related systems are those of Hinch (1984), Joseph *et al.* (1997) and South & Hooper (1999). The results relevant to the present work may be summarized as follows. At low to moderate Schmidt numbers, channel flow is stabilized significantly when the viscosity decreases towards the wall and destabilized when the near-wall fluid is more viscous than that at the core. At high Schmidt numbers the existence of a mixed layer of fluid always leads to destabilization, which increases with Schmidt number. As one would expect, these effects are accentuated with an increase in viscosity contrast. These flows can become absolutely unstable under certain parameter ranges, and the boundary between convective and absolute instabilities has been delineated by Sahu *et al.* (2009). Pipe flow, on the other hand can, when the viscosity contrast is very large, be destabilized even when the less-viscous fluid is at the wall (Selvam *et al.* 2007). In a numerical study of pressure-driven, non-isothermal miscible displacement of one fluid by another in a horizontal channel, Sahu, Ding & Matar (2010) find that increase in viscous heating accelerates the displacement of the resident fluid.

In an SC system, both stabilization and destabilization are far larger (see, e.g., Govindarajan, L'vov & Procaccia 2001) when the critical layer of the dominant eigenmode, i.e. the layer where disturbance production is highest, overlaps with the viscosity stratified layer. We find that such overlap makes the new DD mode of instability stronger as well, and we distinguish this mode from the overlap mode of SC systems.

2. Formulation

The linear stability analysis of pressure-driven three-layer flow of two miscible, Newtonian and incompressible fluids of equal density and different viscosities in a horizontal, planar channel is considered. The fluid in the channel core (fluid 1) may be taken to be a pure solvent. The outer fluid (fluid 2) differs from the inner in that it contains the same solvent, but has in it two solute species, F and S, where F diffuses faster than S, at fixed concentrations. The ratio δ of the respective diffusion rates $\mathscr{D}_f$ and $\mathscr{D}_s$ is $\geqslant 1$ by definition. In between there is a mixed layer of thickness q. Note that one of the 'solutes' could even be temperature, so we

https://doi.org/10.1017/jfm.2011.388 Published online by Cambridge University Press

use the general term 'scalar' to describe them. We use the Cartesian coordinate system where x and y denote the horizontal and vertical coordinates, respectively. The channel walls, which are rigid and impermeable, are located at $y = \pm H$. The flow dynamics is governed by the continuity and Navier–Stokes equations, in addition to two convection–diffusion equations for the two scalars. We assume an exponential dependence on the concentration of the viscosity, μ:

$$\mu = \mu_1 \exp\left[R_s\left(\frac{S - S_1}{S_2 - S_1}\right) + R_f\left(\frac{F - F_1}{F_2 - F_1}\right)\right], \tag{2.1}$$

where $R_s(\equiv (S_2 - S_1)\,\mathrm{d}(\ln\mu)/\mathrm{d}S)$ and $R_f(\equiv (F_2 - F_1)\,\mathrm{d}(\ln\mu)/\mathrm{d}F)$ are the log-mobility ratios of the scalars S and F, respectively. The following scaling is employed to render the governing equations dimensionless:

$$(x, y) = H(\widetilde{x}, \widetilde{y}), \quad (q, h) = H(\widetilde{q}, \widetilde{h}), \quad t = \frac{H^2}{Q}\widetilde{t}, \quad (u, v) = \frac{Q}{H}(\widetilde{u}, \widetilde{v}), \tag{2.2}$$

$$p = \frac{\rho Q^2}{H^2}\widetilde{p}, \quad \mu = \widetilde{\mu}\mu_1, \quad \widetilde{s} = \frac{S - S_1}{S_2 - S_1}, \quad \widetilde{f} = \frac{F - F_1}{F_2 - F_1}, \tag{2.3}$$

where Q denotes the total volume flow rate per unit distance in the spanwise direction, $u \equiv (u, v)$ is the velocity vector, u and v being its components in the x and y directions, respectively, ρ is the constant density, t is time and p denotes pressure. The tildes here designate dimensionless quantities, but are dropped for convenience in the dimensionless governing equations, given by

$$\nabla \cdot u = 0, \tag{2.4}$$

$$\left[\frac{\partial u}{\partial t} + u \cdot \nabla u\right] = -\nabla p + \frac{1}{Re}\nabla \cdot [\mu(\nabla u + \nabla u^{\mathrm{T}})], \tag{2.5}$$

$$\frac{\partial s}{\partial t} + u \cdot \nabla s = \frac{1}{Pe}\nabla^2 s, \tag{2.6}$$

$$\frac{\partial f}{\partial t} + u \cdot \nabla f = \frac{\delta}{Pe}\nabla^2 f, \tag{2.7}$$

The Reynolds number is defined as $Re \equiv \rho Q/\mu_1$, the Péclet number is defined based on the slower diffusing species as $Pe \equiv Q/\mathscr{D}_s$ and $Sc \equiv Pe/Re$. The effective Schmidt number of the faster diffusing fluid is Sc/δ.

2.1. *Base state*

The base state, about which linear stability characteristics will be analysed, corresponds to a steady, parallel, fully developed flow. Base state quantities are designated by uppercase letters, as in the case of U, V and P, which are the streamwise and wall normal velocity components and pressure, respectively, and by the subscript 0 for viscosity, s and f. Here $V = 0$, U is a function of y alone and P is linear in x. A schematic of the system is shown in figure 1. Since the mixed layer is diffusing very slowly, with a divergence angle scaling as Pe^{-1}, we may consider it, to a very good approximation, to be of constant thickness locally, and therefore the flow as locally parallel. In an experiment, to obtain such a base state, one would need a long channel, and a careful inlet design. For $Sc \gg 1$ momentum would diffuse far sooner than concentration and over a long length of the channel we would have profiles of the type shown in the figure, with a thin mixed layer. An identical profile for both solutes, on the other hand, may not be easy to achieve, since the faster

https://doi.org/10.1017/jfm.2011.388 Published online by Cambridge University Press

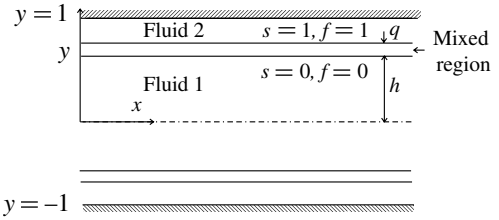


FIGURE 1. Schematic of the three-layer base state flow. The fluids 1 and 2 occupy the channel core and the region adjacent to the channel walls, respectively. The two fluids are separated by a mixed layer of uniform thickness q, with fluid 1 located in the region $-h \leqslant y \leqslant h$.

diffusing fluid will have a correspondingly thicker mixed layer. Our primary objective here is however to bring out the effect of different diffusivities on the disturbance growth alone. To isolate this physics we prescribe identical mean concentration profiles for the two solutes, and show that there is a new DD mode of instability even in this case. We have made computations for a realistic thickness ratio as well (not shown) and find the DD instability to be significantly enhanced. The two constant property fluids are thus separated by a mixed layer of uniform thickness q, with fluid 1 located in the region $-h \leqslant y \leqslant h$ and fluid 2 in the region $h + q <\mid y \mid< 1$.

For the base flow we prescribe a symmetry boundary condition across the centreline. The scalars s_0 and f_0 are chosen to be fifth-order polynomials in the mixed layer, as shown below, such that the concentrations are continuous up to the second derivative at $y = h$ and $y = h + q$:

$$s_0 = f_0 = 0, \quad 0 \leqslant y \leqslant h, \tag{2.8a}$$

$$s_0 = f_0 = \sum_{i=1}^{6} a_i y^{i-1}, \quad h \leqslant y \leqslant h + q, \tag{2.8b}$$

$$s_0 = f_0 = 1, \quad h + q \leqslant y \leqslant 1, \tag{2.8c}$$

where a_i $(i = 1, 6)$ are given by

$$a_1 = -\frac{h^3}{q^5}(6h^2 + 15hq + 10q^2), \quad a_2 = \frac{30h^2}{q^5}(h + q)^2, \tag{2.9a}$$

$$a_3 = -\frac{30h}{q^5}(h + q)(2h + q), \quad a_4 = \frac{10}{q^5}(6h^2 + 6hq + q^2), \tag{2.9b}$$

$$a_5 = -\frac{15}{q^5}(2h + q) \quad \text{and} \quad a_6 = \frac{6}{q^5}. \tag{2.9c}$$

We have confirmed that other sufficiently smooth profiles will give results practically indistinguishable from those presented here. Solving the steady, fully developed version of (2.5), i.e.

$$Re\left(\frac{\mathrm{d}P}{\mathrm{d}x}\right) = \frac{\mathrm{d}}{\mathrm{d}y}\left(\mu_0 \frac{\mathrm{d}U}{\mathrm{d}y}\right), \tag{2.10}$$

subject to no-slip and no-flux conditions at the wall and the centreline of the channel, respectively, we obtain the base state velocity profile, $U(y)$. Here $\mu_0 = \mathrm{e}^{(R_s s_0 + R_f f_0)}$. The non-dimensional pressure gradient $\mathrm{d}P/\mathrm{d}x$ is fixed by using $\int_0^1 U \,\mathrm{d}y = 1$.

https://doi.org/10.1017/jfm.2011.388 Published online by Cambridge University Press

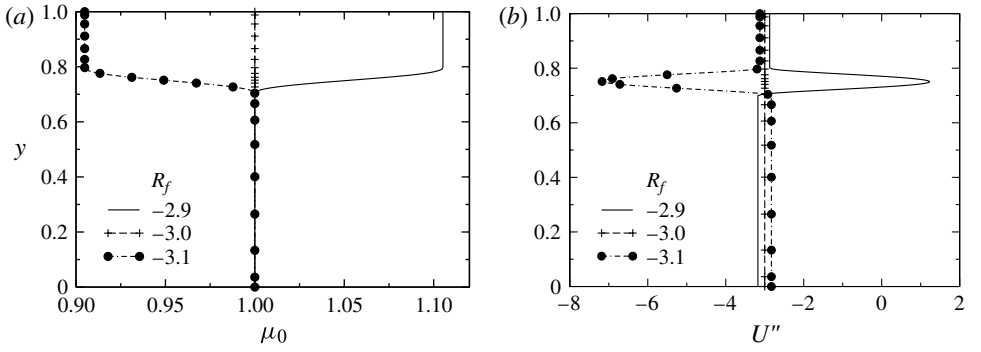


FIGURE 2. Basic steady-state profiles of (*a*) viscosity (*b*) second derivative of the streamwise velocity, for different values of R_f. The other parameters are chosen as $h = 0.7$, $q = 0.1$, $Re = 200$ and $R_s = 3$.

Typical base state profiles of the viscosity and the second derivative of the horizontal velocity component (U'') are shown in figure 2(*a*,*b*), respectively, for different R_f. For $R_s = 3$, the viscosity of fluid 2 is higher and lower as compared with fluid 1 for R_f equal to -2.9 and -3.1, respectively; $R_s = -R_f$ being a case when both the fluids have the same viscosity. Therefore, with $R_f = -2.9$ we have destabilization, while $R_f = -3.1$ gives a profile which may be denoted as 'stably stratified' with respect to viscosity. An inspection of figure 2(*b*) reveals that the profile becomes inflectional (undergoes $U'' = 0$ at some point) for $R_f = -2.9$, indicating by Rayleigh's theorem that the flow is inviscidly unstable (Rayleigh 1880). In the present study our primary interest is in the opposite case (e.g. $R_f = -3.1$) which is inviscidly stable in the sense of Rayleigh, and where we expect the flow to be stabilized compared with a constant viscosity fluid.

2.2. *Linear stability analysis*

We examine the temporal linear stability of the base flow given by (2.8)–(2.10) using a normal modes analysis. In the standard way (see, e.g., Schmid & Henningson 2001) flow variables are split into base state quantities and two-dimensional perturbations, designated by a hat:

$$(u, v, p, s, f)(x, y, t) = (U(y), 0, P, s_0(y), f_0(y)) + (\hat{u}, \hat{v}, \hat{p}, \hat{s}, \hat{f})(y)\mathrm{e}^{\mathrm{i}(\alpha x - \omega t)}, \quad (2.11)$$

such that a given mode is unstable if $\omega_i > 0$, stable if $\omega_i < 0$ and neutrally stable if $\omega_i = 0$. Here $\mathrm{i} \equiv \sqrt{-1}$, α and $\omega(\equiv \alpha c)$ are the wavenumber (real) and frequency (complex) of the disturbance, respectively, wherein c is the phase speed of the disturbance. In (2.11), the perturbation viscosity is given by $\hat{\mu} = (\partial\mu_0/\partial s_0)\hat{s} + (\partial\mu_0/\partial f_0)\hat{f}$. The amplitude of the velocity disturbances are then re-expressed in terms of a streamfunction ($(\hat{u}, \hat{v}) = (\psi', -\mathrm{i}\alpha\psi)$); the prime denotes differentiation with respect to y. Substitution of (2.11) into (2.4)–(2.7), subtraction of the base state equations, subsequent linearization and elimination of the pressure perturbation yields the following linear stability equations (Drazin & Reid 1985; Govindarajan 2004), where the hat notation is suppressed:

$$\begin{aligned}\mathrm{i}\alpha Re[(\psi'' - \alpha^2\psi)(U - c) - U''\psi] = \mu_0\left(\psi^{iv} - 2\alpha^2\psi'' + \alpha^4\psi\right)\\ + 2\mu_0'(\psi''' - \alpha^2\psi') + \mu_0''(\psi'' + \alpha^2\psi)\\ + U'(\mu'' + \alpha^2\mu) + 2U''\mu' + U'''\mu, \end{aligned} \quad (2.12)$$

https://doi.org/10.1017/jfm.2011.388 Published online by Cambridge University Press

$$\mathrm{i}\alpha Pe[(U-c)s-\psi s_0']=(s''-\alpha^2 s), \tag{2.13}$$

$$\mathrm{i}\alpha Pe[(U-c)f-\psi f_0']=\delta(f''-\alpha^2 f). \tag{2.14}$$

Solutions of these equations are obtained subject to the boundary conditions

$$\psi=\psi'=s=f=0 \quad \text{at } y=1, \tag{2.15}$$

and

$$\psi'=\psi'''=s'=f'=0 \quad \text{at } y=0 \text{ (sinuous mode)}, \tag{2.16}$$

or

$$\psi=\psi''=s=f=0 \quad \text{at } y=0 \text{ (varicose mode)}. \tag{2.17}$$

We found for the range of parameters considered that the sinuous mode is dominant and therefore present results exclusively for this mode.

Equations (2.12)–(2.14) along with the boundary conditions (2.15)–(2.17) constitute an eigenvalue problem which is discretized using Chebyshev spectral collocation (Canuto *et al.* 1987) and solved using the public domain software, LAPACK. As gradients are large in the mixed region, we require a large number of grid points in this region. For this we use the stretching function (Govindarajan 2004)

$$y_j=\frac{a}{\sinh(by_0)}[\sinh\{(y_c-y_0)b\}+\sinh(by_0)], \tag{2.18}$$

where y_j are the locations of the grid points, a is the midpoint of the mixed layer, y_c is a Chebyshev collocation point, defined as $y_c=0.5\cos\{[(\pi(j-1)/(n-1))]+1\}$, where n is the number of collocation points, taken to be 121 in this study,

$$y_0=\frac{0.5}{b}\ln\left[\frac{1+(\mathrm{e}^b-1)a}{1+(\mathrm{e}^{-b}-1)a}\right], \tag{2.19}$$

and b is the degree of clustering. We have taken $b=8$ which gives an accuracy of at least five decimal places in the range of parameters used.

3. Results and discussion

We begin by ensuring that 121 collocation points are sufficient for obtaining accurate eigenvalues. We also confirm that the neutral stability curve for a single fluid channel flow, obtained by setting $R_s=0$ and $R_f=0$ in the present formulation, agrees completely with the standard result. Based on the mass flux Q, our critical Reynolds number, Re_{cr}, for this case is 3848.16, which is two-thirds of the more commonly quoted value of 5772.2 based on the maximum velocity (Drazin & Reid 1985). As a stricter validation exercise, we repeat the computations of Govindarajan (2004). For this we fix $R_f=0$, so the component f drops out of the system and we have a single solute in the annular region, with a mixed layer between $y=h$ and $y=h+q$, as in the earlier study. Sample results are shown in figure 3, which are identical to figure 2 of Govindarajan (2004). The two codes have been developed independently and the mean viscosity is taken to vary exponentially in the present case, but is fitted by a fifth-order polynomial in the older paper. Note the three modes of instability in the figure, the Tollmien–Schlichting (*TS*) mode on the bottom right, the inflexional mode (*I*) on the top right and, more importantly, the relatively low Reynolds number mode on the left which was termed the 'overlap' mode (*O*) to denote the instability arising out of the overlap of the critical layer of the dominant instability with the layer of varying viscosity. The critical layer may be described

https://doi.org/10.1017/jfm.2011.388 Published online by Cambridge University Press

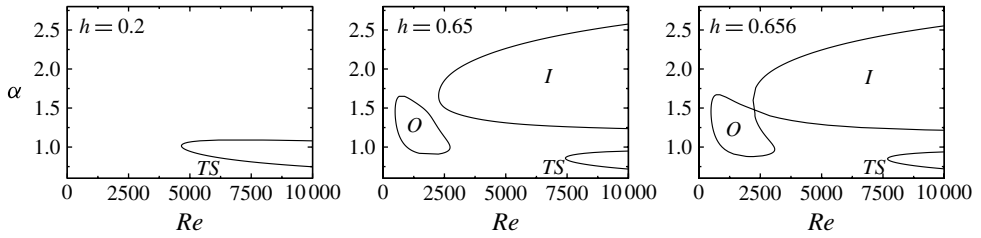


FIGURE 3. Stability boundaries for $q = 0.1$, $Sc = 0$, $R_s = 0.1823$ and $R_f = 0$. These figures are in excellent agreement with Govindarajan (2004).

as follows: associated with a particular disturbance eigenmode is a critical location y_c at which the base flow velocity equals the phase speed ($U = c$ at $y = y_c$). In the critical layer, of thickness $\epsilon \sim Re^{-1/3}$ around y_c, viscous effects are important at any Reynolds number (Lin 1945), and in a region of thickness $\epsilon_c \sim Pe^{-1/3}$ within it, solute diffusion effects are important at any Péclet number. As mentioned above, most of the disturbance kinetic energy is produced here. For this case $y_c = 0.7$. It is seen that the O mode does not exist when the mixed layer is located far away from the critical layer. The O and I modes are seen to merge at $h = 0.656$, and at higher values of h appear as one large region of instability.

In this configuration, viscosity increases towards the wall. It is well documented for an SC fluid (e.g. Hinch 1984) that such a stratification is always destabilizing, whereas a viscosity stratification with viscosity decreasing towards the wall at low Schmidt numbers would typically be stabilizing. Note that for the range of parameters studied, the O mode does not exist when the viscosity is stably stratified, i.e. lower at the wall than at the core.

In figure 4(a), the DD system is compared with a SC system whose diffusivity is the average of $\mathscr{D}_s$ and $\mathscr{D}_f$. There is no instability in SC. However there is a new instability in the case of the DD system. A related study, shown in figure 4(b) is the effect of varying the ratio, δ, of the diffusivity of the faster diffusive component to that of the slower diffusing one. When $\delta = 1$, we have effectively an SC system and we see that the flow is stable. As δ increases, the Schmidt number of the faster diffusing component decreases. From our experience with an SC system, we expect that the reduced effective Schmidt number should result in a stabler flow. What we see in the DD case is counter to these expectations. A decrease in δ actually results in instability.

Figure 5 makes several points. First, it is seen that the DD mode has an identity distinct from the TS mode. More importantly, the DD mode is also distinct from the O mode of an SC fluid. Note the sign change in viscosity stratification between figures 3 and 5. The O mode only appears when the more viscous fluid is close to the wall, i.e. when the viscosity is unstably stratified, whereas the special feature of a DD mode is that it destabilizes a 'stably' stratified flow. In figure 5 the corresponding stability boundary for an SC fluid is also shown. It is clear that there is only a TS mode but no DD mode of instability in that case. The mechanism for the instability in figure 5(a) is broadly analogous to the fingering regime of gravity-driven DD convection. Here the net stratification is stabilizing, with s destabilizing and f stabilizing. Consider a small parcel of fluid displaced vertically. The resulting perturbation in f will diffuse away faster, leaving the destabilizing effect of s, which causes the DD mode. Intuitively less obvious is the existence of DD instability in figure 5(b), where f is destabilizing and s stabilizing. Note that the unstable region, as well as the h range over which

https://doi.org/10.1017/jfm.2011.388 Published online by Cambridge University Press

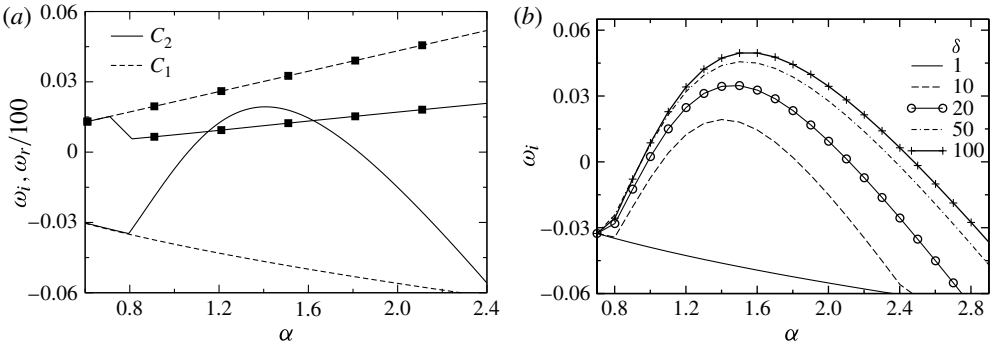


FIGURE 4. (*a*) Comparison of DD with SC stability. Curve C_2, with $Sc = 50$, $R_s = 3$, $R_f = -3.1$ and $\delta = 10$ is for a DD system, while C_1, with $Sc = 9.09$, $R_s = -0.1$, $R_f = 0$ and $\delta = 1$ is for an SC fluid. Lines with and without symbols correspond to variation of ω_r and ω_i with wavenumber, respectively. (*b*) Effect of the relative diffusion rate δ on instability growth rate, $Sc = 50$, $R_s = 3$ and $R_f = -3.1$. For both figures, $h = 0.7$, $q = 0.1$ and $Re = 1000$.

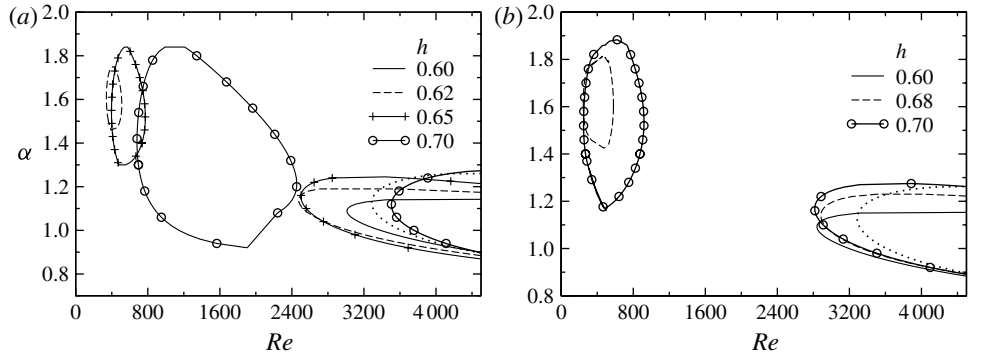


FIGURE 5. Effect of the location h of the viscosity stratification, on the neutral stability boundaries, for (*a*) $R_s = 3$ and $R_f = -3.1$ and (*b*) $R_s = -3.1$ and $R_f = 3$. The other parameters are $q = 0.1$, $Sc = 30$ and $\delta = 10$. The curves on the right are the neutral boundary for the *TS* mode, while the closed curves are those of the DD mode. The dotted line shows the SC result.

it occurs is much smaller than in figure 5(*a*). This case is in broad analogy with the diffusive regime in DD convection (Turner 1974). A displaced parcel would now tend to return to its old position but, due to the diffusing away of the f perturbation and the corresponding decrease in viscosity, would tend to overshoot its original location resulting in an oscillatory instability. Figure 5 also demonstrates that an overlap of the critical layer (located at $y_c \sim 0.7$) with the stratified layer is necessary for the DD mode to be destabilized effectively.

Figure 6(*a*) extends our earlier finding that an increase in δ increases the growth rate of the DD instability, to show that the unstable domain grows as well. An increase in Schmidt number, as seen in figure 6(*b*) serves to decrease the critical Reynolds number, as also happens in SC instability, but the unstable domain of DD shrinks unlike in SC. At $Sc = 0$, we should not, and do not, have a DD instability. We have discussed one typical value of R_s and R_f thus far. What happens when the viscosity stratification is smaller? In figure 7(*a*) we show the critical Reynolds number when $R_s = 1$, with the region above each curve being unstable. Here the DD mode does not

https://doi.org/10.1017/jfm.2011.388 Published online by Cambridge University Press

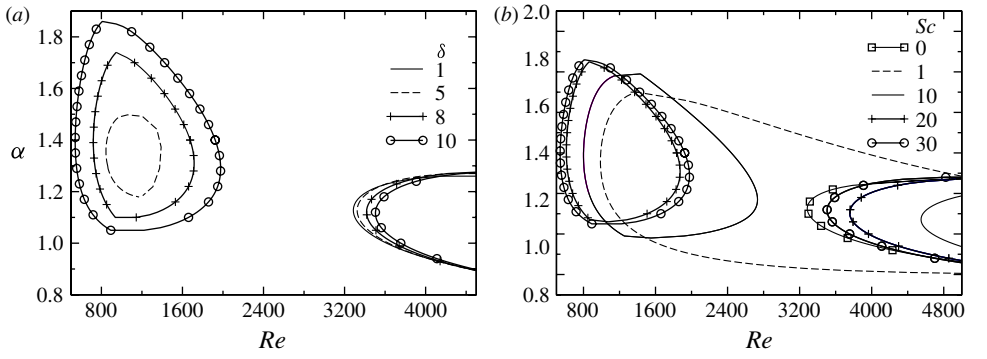


FIGURE 6. Effect of (*a*) δ for $Sc = 30$ and (*b*) Sc for $\delta = 10$ on stability, with $h = 0.7$, $q = 0.1$, $R_s = 3$ and $R_f = -3.1$. Note in panel (*a*) that the DD mode disappears for $\delta = 1$.

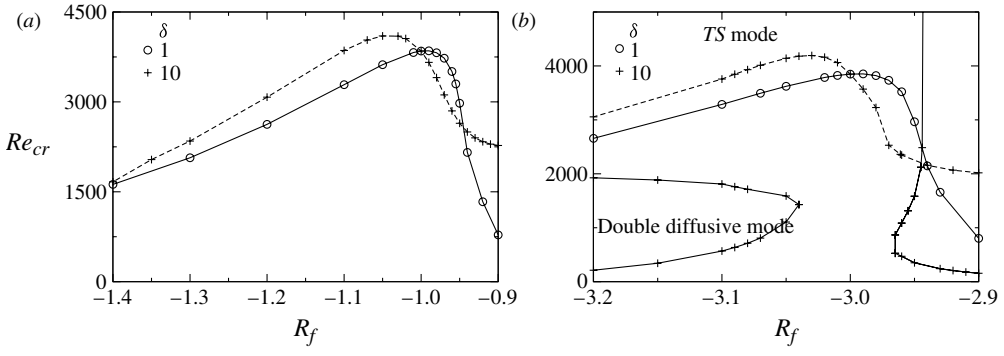


FIGURE 7. Effect of R_f on the critical Reynolds number for (*a*) $R_s = 1$ and (*b*) $R_s = 3$. For $R_f > -3$ we see an unstable region to the right of the solid line, resulting from the overall destabilizing viscosity stratification. We fix $h = 0.7$, $q = 0.1$ and $Sc = 50$.

go unstable, and stability is decided by the modified *TS* mode. When $R_f = -1$ we have unstratified fluid, with an $Re_{cr} = 3848.16$ for any δ. Since the Schmidt number is high, the *TS* mode is destabilized by a net viscosity stratification of either sign. Making the system DD, i.e. increasing δ from 1 to 10, does not change the TS answer qualitatively. However, when the overall viscosity stratification is increased, it is seen in figure 7(*b*) that while the modified *TS* mode is still unaffected qualitatively, the new DD mode appears over a range of R_f.

The viscosity perturbations, resulting from a combination of s and f, can have a richer structure in a DD system, as seen in the sample set of eigenfunctions shown in figure 8, and this provides the mechanism for more interesting dynamics. All of the eigenfunctions peak in the vicinity of the stratified layer, which overlaps with the critical layer of this mode. As δ is increased, we see that s is practically unaffected, but f decreases in amplitude, allowing for s to dominate and thus DD instability to be manifested in this 'stably stratified' system.

4. Conclusion

A DD instability driven by viscosity contrasts in shear flow has been shown to occur. The DD system has been shown to be fundamentally different from the SC system

https://doi.org/10.1017/jfm.2011.388 Published online by Cambridge University Press

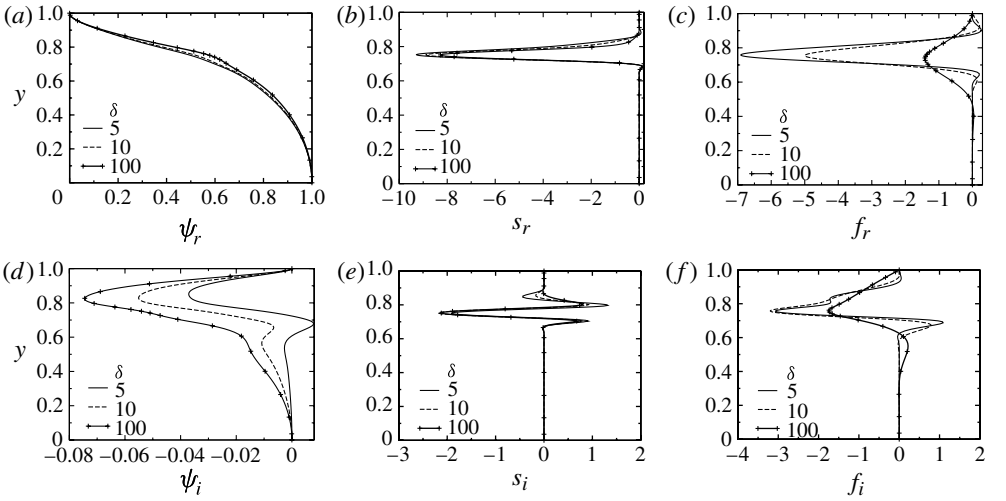


FIGURE 8. Eigenfunctions of ψ, s and f for $Re = 1000$, $\alpha = 1.3$, $q = 0.1$, $Sc = 30$, $R_s = 3$ and $R_f = -3.2$. The subscripts r and i represent the real and imaginary parts of the eigenfunctions.

in terms of its stability characteristics. In particular, unlike the SC instability, the DD instability occurs in a flow that is nominally stably stratified in terms of viscosity. It is well known that the Orr–Sommerfeld equation constitutes a singular perturbation problem in a typical shear flow, with viscous effects having a large effect in the critical layer. That the critical layer is also important in a viscosity-stratified flow and that a viscosity stratification located here has a far larger effect than one located elsewhere has been analysed in detail before (Govindarajan *et al.* 2001; Govindarajan 2004) and we refrain from a repeat of that analysis here. We mention however that a hierarchy of equations may be derived in the critical layer by expressing all variables as power series in the small parameter ϵ, and the viscosity stratification in the critical layer may be shown to contribute effects at a lower order than elsewhere, and this is evident in the DD system as well. We have performed computations over a range of Reynolds numbers and a variety of other parameters, but have presented only the essence here. We conclude that DD behaviour due to viscosity variation is very interesting and needs further attention.

REFERENCES

CANUTO, C., HUSSAINI, M. Y., QUARTERONI, A. & ZANG, T. A. 1987 *Spectral Methods in Fluid Dynamics*, 1st edn. Springer.

DRAZIN, P. G. & REID, W. H. 1985 *Hydrodynamic Stability*. Cambridge University Press.

ERN, P., CHARRU, F. & LUCHINI, P. 2003 Stability analysis of a shear flow with strongly stratified viscosity. *J. Fluid Mech.* **496**, 295.

GOVINDARAJAN, R 2004 Effect of miscibility on the linear instability of two-fluid channel flow. *Intl J. Multiphase Flow* **30**, 1177–1192.

GOVINDARAJAN, R., L'VOV, S. V. & PROCACCIA, I. 2001 Retardation of the onset of turbulence by minor viscosity contrasts. *Phys. Rev. Lett.* **87**, 174501.

GROSFILS, P, DUBOIS, F., YOURASSOWSKY, C. & DE WIT, A. 2009 Hot spots revealed by simultaneous experimental measurement of the two-dimensional concentration and temperature fields of an exothermic chemical front during finger-pattern formation. *Phys. Rev.* E **79**, 017301.

https://doi.org/10.1017/jfm.2011.388 Published online by Cambridge University Press

HEJAZI, S. H., TREVELYAN, P. M. J., AZAIEZ, J. & DE WIT, A. 2010 Viscous fingering of a miscible reactive $a + b \rightarrow c$ interface: a linear stability analysis. *J. Fluid Mech.* **652**, 501–528.

HINCH, E. J. 1984 A note on the mechanism of the instability at the interface between two shearing fluids. *J. Fluid Mech.* **144**, 463–465.

HUPPERT, H. E. 1971 On the stability of a series of double-diffusive layers. *Deep-Sea Res. Oceanogr. Abstr.* **18** (10), 1005–1021.

JOSEPH, D. D., BAI, R., CHEN, K. P. & RENARDY, Y. Y. 1997 Core-annular flows. *Ann. Rev. Fluid Mech.* **29**, 65.

LIN, C. C. 1945 On the stability of two dimensional parallel flows Part III – stablilty in a viscous fluid. *Q. Appl. Maths* **III**, 277–301.

MALIK, S. V. & HOOPER, A. P. 2005 Linear stability and energy growth of viscosity stratified flows. *Phys. Fluids* **17**, 024101.

MAY, B. D. & KELLEY, D. E. 1997 Effect of baroclinicity on double-diffusive interleaving. *J. Phys. Oceanogr.* **27**, 1997–2008.

MISHRA, M, TREVELYAN, P. M. J., ALMARCHA, C & DE WIT, A. 2010 Influence of double diffusive effects on miscible viscous fingering. *Phys. Rev. Lett.* **105**, 204501.

NAGATSU, Y., MATSUDA, K., KATO, Y. & TADA, Y. 2007 Experimental study on miscible viscous fingering involving viscosity changes induced by variations in chemical species concentrations due to chemical reactions. *J. Fluid Mech.* **571**, 475–493.

PODGORSKI, T, SOSTARECZ, M. C., ZORMAN, S & BELMONTE, A 2007 Fingering instabilities of a reactive micellar interface. *Phys. Rev.* E **76**, 016202.

PRITCHARD, D. 2004 The instability of thermal and fluid fronts during radial injection in a porous medium. *J. Fluid Mech.* **508**, 133–163.

PRITCHARD, D. 2009 The linear stability of double-diffusive miscible rectilinear displacements in a Hele-Shaw cell. *Eur. J. Mech. (*B*/Fluids)* **28** (4), 564–577.

RANGANATHAN, B. T. & GOVINDARAJAN, R. 2001 Stabilisation and destabilisation of channel flow by location of viscosity-stratified fluid layer. *Phys. Fluids* **13** (1), 1–3.

RAYLEIGH, L. 1880 On the stability of certain fluid motions. *Proc. Lond. Math. Soc.* **11**, 57–70.

SAHU, K. C., DING, H. & MATAR, O. K. 2010 Numerical simulation of non-isothermal pressure-driven miscible channel flow with viscous heating. *Chem. Engng Sci.* **65**, 3260–3267.

SAHU, K. C., DING, H., VALLURI, P. & MATAR, O. K. 2009 Linear stability analysis and numerical simulation of miscible channel flows. *Phys. Fluids* **21**, 042104.

SCHMID, P. J. & HENNINGSON, D. S. 2001 *Stability and Transition in Shear Flows*. Springer.

SELVAM, B, MERK, S, GOVINDARAJAN, R & MEIBURG, E 2007 Stability of miscible core-annular flows with viscosity stratification. *J. Fluid Mech.* **592**, 23–49.

SOUTH, M. J. & HOOPER, A. P. 1999 Linear growth in two-fluid plane Poiseuille flow. *J. Fluid Mech.* **381**, 121–139.

SWERNATH, S & PUSHPAVANAM, S 2007 Viscous fingering in a horizontal flow through a porous medium induced by chemical reactions under isothermal and adiabatic conditions. *J. Chem. Phys.* **127**, 204701.

TURNER, J. S. 1974 Double-diffusive phenomena. *Annu. Rev. Fluid Mech.* **6**, 37–54.

https://doi.org/10.1017/jfm.2011.388 Published online by Cambridge University Press